minerals

MDPI

Article

N_2 and CO_2 Adsorption by Soils with High Kaolinite Content from San Juan Amecac, Puebla, México

Karla Quiroz-Estrada [1], Miguel Ángel Hernández-Espinosa [1,*], Fernando Rojas [2], Roberto Portillo [3], Efraín Rubio [4] and Lucía López [5]

1 Zeolites Research Department and Postgraduate in Sustainable Management of Agroecosystems, Autonomous University of Puebla, Puebla City 72570, Mexico; k.quiroz.estrada@gmail.com
2 Department of Chemistry, Autonomous Metropolitan University, Iztapalapa, Ciudad de México 09340, Mexico; fernando@xanum.uam.mx
3 Faculty of Chemistry, Autonomous University of Puebla, Puebla City 72570, Mexico; efrainrubio@yahoo.com
4 University Center of Linking and Technology Transfer, Autonomous University of Puebla, Puebla City 72570, Mexico; portilloreyes@yahoo.com
5 Soils Microbiology Laboratory, Autonomous University of Puebla, Puebla City 72570, Mexico; lucia.lopez@correo.buap.mx
* Correspondence: vaga1957@gmail.com; Tel.: +54-222-229-5500 (ext. 7270)

Academic Editor: Tuncel M. Yegulalp
Received: 8 March 2016; Accepted: 17 June 2016; Published: 14 July 2016

Abstract: Carbon dioxide (CO_2) is considered one of the most important greenhouse gases in the study of climate change. CO_2 adsorption was studied using the gas chromatography technique, while the Freundlich and Langmuir adsorption models were employed for processing isotherm data in the temperature range of 473–573 K. The isosteric heat of adsorption was calculated from the Clausius–Clapeyron equation. Moreover, the thermodynamic properties ΔG, ΔU, and ΔS were evaluated from the adsorption isotherms of Langmuir using the Van't Hoff Equation. The four soil samples were recollected from San Juan Amecac, Puebla, Mexico, and their morphologies were investigated through X-ray diffraction (XRD) and N_2 adsorption at 77 K. The SJA4 soil has a crystalline Kaolinite phase, which is one of its non-metallic raw materials, and N_2 isotherms allowed for the determination of pore size distributions and specific surface areas of soil samples. The Barrett–Joyner–Halenda (BJH) distribution of pore diameters was bimodal with peaks at 1.04 and 3.7 nm, respectively. CO_2 adsorption showed that the SJA1 soil afforded a higher amount of adsorbed CO_2 in the temperature range from 453 to 573 K followed by SJA4 and finally SJA2, classifying this process as exothermic physisorption.

Keywords: adsorption; soils; CO_2; N_2; kaolinite; isosteric heat; Freundlich; Brunauer-Emmett-Teller (BET) approach

1. Introduction

Nowadays. one problem that affects our society is the treatment of greenhouse gases, namely, the enforcement of a separation, capture, and storage that is environmentally friendly and economically viable [1], particularly CO_2 given that this gas is becoming increasingly important in the future of the world economy [2]. Carbon dioxide (CO_2) is considered one of the main greenhouse gases producing global warming. Hence, the adsorption processes require the development of new technologies for the effective adsorption and storage of large amounts of CO_2 [3]. Carbon sequestration means capturing CO_2 from the atmosphere or from anthropogenically produced large-scale mixtures of effluent gases exhausted from industries. On the other hand, carbon capture involves the separation of this compound from a gas mixture and to adsorb (concentrate) it on the surface of assorted substrates.

CO_2 is particularly important for its effect on the climate conditions of the planet, since it is a long-standing gas that remains active in the atmosphere for a long time. Once the CO_2 reaches the atmosphere, it reacts immediately with the short-lived gases of the biosphere and surface ocean, and the remaining CO_2 remains for hundreds of years to be captured and converted amid the deep ocean and the terrestrial biosphere [4]. Between 2000 and 2006, CO_2 sink by land accounted for about 0.30 of the total airborne fraction; while the ocean sink accounted for 0.24 and the atmospheric accumulation of the gas amounted to 0.45 [5].

A special feature of contaminant sorption by soils is that it is a multiple reaction phenomenon. Most natural soils are inherently heterogeneous, including the microscopic-scale soils, due to the fact that their composition and framework are variable at interparticle and intraparticle scale [6]. The ideal adsorption of molecules in pore systems depends on the pore character in relation to its shape, size, and chemical nature [7]. Any solid can fix or adsorb on the surface, molecules, atoms, or ions. In the area of gas–solid interfaces, the use of sorption isotherms is widely spread to determine the adsorption capacity of the substrate [8].

Soils are considered complex systems, a mixture primarily composed of organic matter and mineral material such as quartz and clay; quartz is completely inert, organic matter, and clays expand when exposed to water and other fluids, thereby increasing the surface area and adsorption capacity. Carbon dioxide capture and storing (CCS) occur in three steps: CO_2 is separated from other industrial mixture gases when it is captured at its source, CO_2 is stored away in the atmosphere in a compressed form to a suitable storage location, i.e., underground, the deep ocean, or in some mineral compounds. During the last few years, certain commercial projects have already been developed for CO_2 storage in underground geological formations, such as oil and gas recovery and abstraction projects [9].

The presence of kaolinite clays in earth soils can strongly affect the mass-transfer processes occurring in natural environments [10]. Kaolinite is a mineral solid that consists of tetrahedral silicate sheets and octahedral hydroxide sheets in a 1:1 proportion [11]. The mass transfer that takes place in the environment process can be significantly affected by the presence of kaolinite clays in soils. Usually, if pollutants are originated in different sources such as domestic sewage, sludge, and other solid waste, and these are poured on the earth surface, the mineral particles of soils react with them. In this way, the presence of clay minerals in soils acts as pollutant collectors improving the environment [12].

The amount of CO_2 adsorbed by adsorbents is dependent on temperature, CO_2 partial pressure, and the potential interaction between CO_2 and the adsorbent itself [13], as well as the topography of the adsorbent surface. Adsorption is considered one of the most promising physical processes used by new technologies to efficiently capture CO_2 from flue gases [3]. Adsorption occurs from interactions among the individual atoms, ions, and molecules of an adsorbate and those present on the adsorbent surface. The process involves the separation of a substance from one phase and its accumulation at the surface of another [14].

Adsorption occurs from interactions between the accumulation of individual atoms and molecules of the adsorbate and the surface of the adsorbent. It must separate and accumulate a fluid phase on a solid surface. It is necessary to know the porous system of solids to understand most processes that are carried out on them, such as nutrient dynamics and adsorption phenomena. Environmental chemistry has been of significant importance since organic and inorganic adsorption includes the transport and activity of pollutants in soils, sediments, and water; consequently, it affects the bioavailability, biodegradability, and ultimate destination of organic waste [15,16].

Several adsorption processes are frequently used in the industry, e.g., pressure swing adsorption (PSA) and thermal or temperature swing adsorption (TSA) [16]. The main contrast concerning these processes is that, in PSA, the pressure of the adsorption bed is reduced; on the other hand, in TSA processes, the temperature increases while pressure remains fairly constant. Zeolites are the most common materials used as adsorbents in the study of CO_2 capture by PSA and TSA technologies [17].

The purpose of this work consisted in the evaluation of the total amount of CO_2 adsorbed on four kinds of kaolinite clay soils [18]. This determination can help to establish the efficacy toward CO_2 capture by actual soils. In this respect, kaolinite soils were chosen for this CO_2 adsorption study [19] by virtue of its being the most widespread clay mineral in earth, since entire clay deposits can be composed of this mineral. This kind of soil contains a high amount of colloidal particles and becomes viscous when wet. As a result, the capture of CO_2 by kaolinitic soils should be an interesting subject of research, since, for instance, once captured, CO_2 can remain in storage conditions [20], awaiting further transformation into other compounds. CO_2 adsorption is one of the best methods for measuring the microporosity of a given material. However, the fact that micropores are the smallest of voids, with pore widths less than 2 nm, makes the desorption process of the adsorbate difficult. On the one hand, zeolites are one of the best known microporous substrates and are very useful for performing CO_2 capture. On the other hand, mesoporous solids (soils included) are sometimes preferred since the transport properties are better qualified for a faster uptake and liberation of gases (CO_2 included).

2. Materials and Methods

Four soil samples were collected in the locality of San Juan Amecac, Puebla, Mexico. The geographical location of these soils is 18°50′24″ N and 98°39′23″ W. In each sampling site, of an area of approximately 550 m^2, 5 simple samples of about 1.5 kg were taken and mixed together to form a compound specimen of 7.5 kg in total, of which 1 kg was taken for characterization purposes. This same sampling process was repeated for each soil, and every 1 kg specimen was then dried under sunlight and sieved at a mesh size of 0.3–0.18 mm. Samples were labeled as SJA1, SJA2, SJA3 and SJA4, respectively.

2.1. X-Ray Diffraction (XRD) and Energy-Dispersive X-Ray Spectroscopy (EDS)

XRD patterns were determined through a Bruker D8 diffractometer using nickel-filtered Cu Kα (λ = 0.154 nm) radiation operated at 40 kV and 30 mA [8]. The crystalline phases were identified by comparing the diffraction patterns obtained with the database of the International Centre for Diffraction Data (ICDD) (JCPDS-ICDD, 2000). The samples were scanned within the range of 5°–60° 2θ with a step size of 0.03 2θ and a counting time of 2 s. In turn, EDS (Energy-Dispersive X-Ray Spectroscopy) analyses were performed in a JEOL JSM-6610LV instrument (Jeol Ltd., Tokyo, Japan) equipped with a tungsten filament electron detector operated at 30 kV. This allowed for the obtainment of the elemental composition at the nanoscopic level.

2.2. N_2 Adsorption

N_2 adsorption isotherms were carried out at the boiling point of liquid nitrogen (76 K) at an altitude of 2200 m in Puebla City, México (2200 m above mean sea level AMSL), using an automatic volumetric adsorption instrument (Quantachrome AutoSorb-1C, Quantachrome Instruments, Boynton Beach, FL, USA). This equipment includes, in addition to the mechanical pump, a turbomolecular pump and a low-pressure transducer, which is located close to the measuring adsorption cell. N_2 adsorption isotherms were evaluated at the relative pressure range (p/p^0) of 10^{-6}–1. Where p is the adsorption pressure and p^0 is the saturation pressure at 76 K of N_2. A specific mesh size of 0.250 mm was used for all samples. Before carrying out the experimental run, the samples were degassed via thermal treatments at 623 K for 20 h under a vacuum of 10^{-5} Torr [21]. Pore size distribution (PSD) was calculated by the Barrett–Joyner–Halenda (BJH) method, applied to the N_2 adsorption boundary isotherm.

2.3. CO_2 Adsorption

The adsorption properties of the soils were further evaluated by means of a GOW-MAC 350 gas chromatograph (GOW-MAC Instrument Co., Bethlehem, PA, USA) provided with a thermal conductivity detector (TCD). Soil samples were packed into the stainless steel columns with a diameter

of 5 mm and a length of 50 cm. Soils were outgassed in situ with a helium flow as carrier gas for 3 h at 573 K. Retention times were measured within the temperature range of 573–453 K, and from these the adsorption isotherms were determined through the chromatographic technique (i.e., the GC peak maxima method) [22].

Structural changes of the soil specimens begin with their endothermic dehydroxylation to metastable metakaolinite phases, occurring from 723 to 973 K [23].

2.4. Data Analysis

Mathematical models of Freundlich and Langmuir were using for the analysis of the CO_2 isotherm data.

Freundlich's isotherm linear form is as follows:

$$\ln a = \ln K_F + \frac{1}{n} \ln p \ (n > 1), \tag{1}$$

where a is the amount of CO_2 adsorbed by the soil samples expressed in mmoles at pressure p, followed by K_F, which is the Freundlich adsorption constant; and n is an exponential factor. In this approach, the Henry constant (K_H) were evaluated for the soils under study according to the following expression:

$$K_H = \lim_{P \to 0} \left(\frac{a}{a_m p} \right). \tag{2}$$

Langmuir equation in its linear form is given as

$$\frac{1}{a} = \frac{1}{a_m} + \left(\frac{1}{a_m K_L} \cdot \frac{1}{P} \right), \tag{3}$$

where a_m is the monolayer capacity, and K_L is the Langmuir adsorption constant.

3. Results and Discussion

3.1. Crystalline Phases and Chemical Composition

The XRD (X-ray diffraction) patterns are shown in Figure 1, in which the presence of three crystalline phases has been noted: quartz (Joint Committee on Powder Diffraction Standards, JCPDS card 03-065-0466), albite (JCPDS card 01-071-1150), and kaolinite (JCPDS card 00-001-0527). The sample SJA4 showed a large presence of mineral phases followed by the SJA3, SJA1 and SJA2 materials. The characteristic signals of kaolinite are located at 2θ: 12.04°, 20.09°, 23.7° and 35.65°. This behavior of the obtained XRD patterns are similar to those previously reported [24].

The chemical composition of kaolinite indicates $Al_2Si_2O_5(OH)_4$ structural formula with the following weight contents of 46% SiO_2, 39.5% AlO_3, and 14.0% H_2O [25]. Nevertheless, in natural kaolinites proceeding from soils, this composition is rarely found due to the relatively high amount of impurities, generally present as mixtures of minerals, metal oxides, and organic materials. The chemical compositions of the soil samples studied are shown in Table 1.

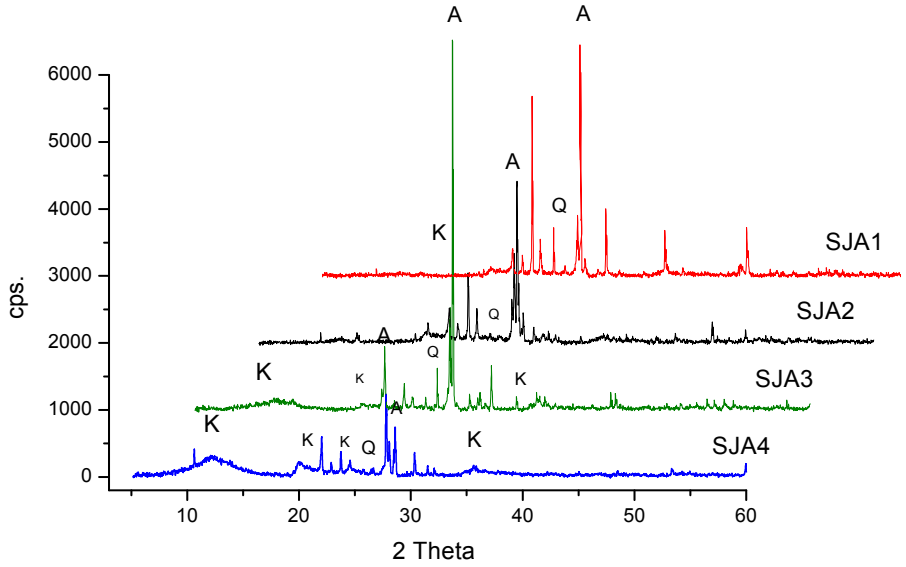

Figure 1. X-ray diffraction (XRD) patterns of soil samples. K = Kaolinite–$Al_2Si_2O_5(OH)_4$, Q = Quartz–SiO_2, A = Albite–$Na(AlSi_3O_8)$.

Table 1. Chemical composition of soil samples.

Compound	SJA1	SJA2	SJA3	SJA4
Na_2O	1.685	2.042	0.517	1.685
MgO	0.000	0.000	4.488	2.338
Al_2O_3	14.191	14.455	10.575	15.211
SiO_2	32.173	44.346	30.148	30.227
K_2O	0.258	0.295	0.000	0.000
CaO	1.994	4.869	0.541	1.758
TiO_2	0.000	1.043	0.323	0.167
Fe_2O_3	4.046	3.710	7.058	3.408
SiO_2/AlO_3 Ratio	2.267	3.068	2.851	1.987

3.2. N_2 Adsorption

The textural parameters of the samples were determined from the N_2 adsorption isotherms of at 76 K (Figure 2).

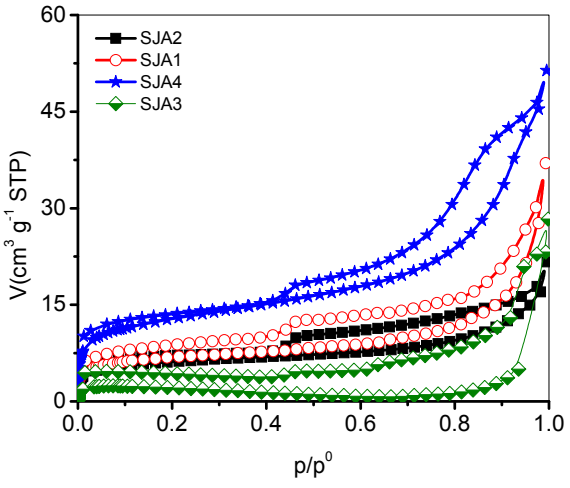

Figure 2. N_2 adsorption isotherms of soil samples from San Juan Amecac, Puebla, México.

The initial part (p/p^0 = 0.1–0.4) of these isotherms can be attributed to the formation of multilayer formation, since it follows the course corresponding to the IUPAC Type II isotherm. Therefore, when N_2 molecules are deposited on mesoporous soils, there surges a competition among the fluids invading the substrate; on the other hand, the intensity of this invasion will be a function of the amount of pores of given sizes and of their surface heterogeneity [21]. In these isotherms, the adsorption is carried out on the pore walls and is similar to the classic way observed in real porous solids with structures in which mesopores dominate.

Based on the shape of the isotherms (IUPAC Type IV and IUPAC type H3 hysteresis loops) that present this type of soil, the Brunauer–Emmet–Teller equation (BET) was satisfactorily applied. The values obtained of the BET constants (C_{BET}) are similar for SJA1, SJA2, and SJA4, whereas the C_{BET} for the SJA3 soil is the smallest of all since the corresponding isotherm shows no definite knee (i.e., the monolayer adsorption is not as definite as with the other samples and the specific surface area is also the smallest of all). Additionally, a negative C_{BET} value indicates a low adsorption energy for the same reason for which the transition from the monolayer adsorption to the multilayer formation is not sharp. All C_{BET} values are higher than unity, something that confirms the absence of micropores. In the same table, by comparison, the values of the pore total volumes, V_Σ, are listed and evaluated according to the Gurvitsch rule at p/p^0 = 0.95. The highest values of the specific surface, the total volume, and the diameter are obtained in the sample SJA4 (Table 2).

Table 2. N_2 adsorption data of soils samples of San Juan Amecac, Puebla, México.

Sample	As_{BET} $m^2 \cdot g^{-1}$	*R*	C_{BET}	BET p/p^0 Plot	V_Σ $cm^3 \cdot g^{-1}$
SJA1	25	0.999	240	0.010–0.131	0.033
SJA2	22.2	0.999	265	0.010–0.164	0.023
SJA3	6.73	0.998	33.24	0.084–0.189	0.034
SJA4	45.9	0.999	270	0.010–0.189	0.064

PSD was calculated from the N_2 adsorption isotherms through BJH analysis (Figure 3), and the results indicated that Sample SJA4 produces bimodal distributions with pore sizes of around 1.043 and 3.790 nm, and SJA3 also shows bimodal distribution but with 3.3- and 5.2-nm values. However, the intensity of these signals depends on the content of kaolinite in soils. In the case of SJA1 and SJA2, unimodal distributions (≈3.6 nm) are produced. According to the size, they are called mesopores that exist in the external area of the soils studied.

The SJA3 sample was found to be poorly consolidated because, at temperatures from 523 to 573 K, it is compacted, and gases such as He and CO_2 cannot pass through the chromatography column, impeding the obtainment of any results. Thus, it was not adapted to the experimental conditions of adsorption of 523–573 K and 517–1034 mm Hg, and, therefore, only the chromatography results of Samples SJA1, SJA2 and SJA4 are shown.

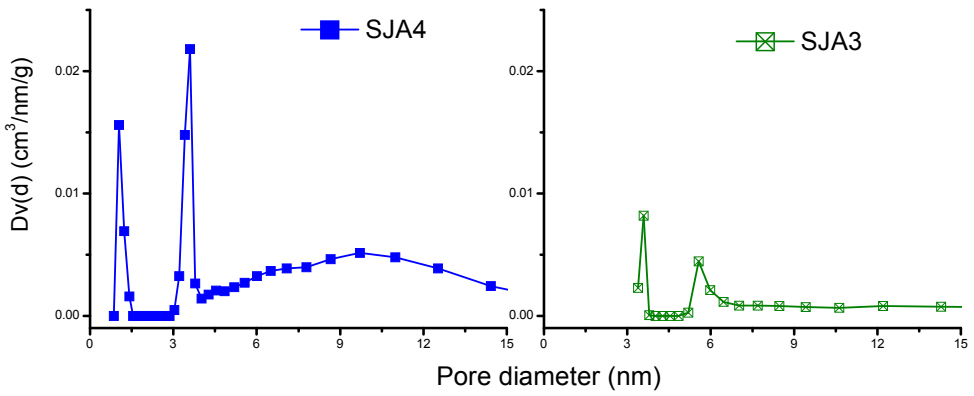

Figure 3. *Cont.*

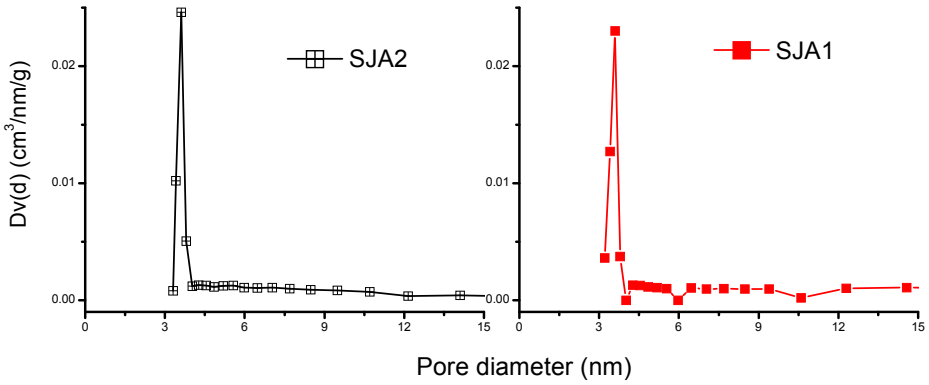

Figure 3. Pore size distribution of soils samples.

3.3. CO_2 Adsorption

The adsorptions isotherms of CO_2 are presented in Figure 4. The nonlinear shape of CO_2 isotherms is more likely to be associated with interactions of CO_2 with high-energy adsorption sites on mineral surfaces [5]. Sample SJA2 presents the lowest adsorption capacity with maximum values of 0.055 mmol/g at higher pressures in comparison with the other soil samples, while Sample SJA1 presents the highest quantity of substance adsorbed with 0.106 mmol/g. These results are higher than those obtained either for natural clinoptilolites (zeolites) or for similar specimens treated chemically, with values of the total adsorbed CO_2 mass amounting to 0.06–0.09 mmol/g [21]. The CO_2 retention at 298 K in HDP–montmorillonite (clay) (0.038–0.06 mmol/g) [26] and Skardon River kaolinite (0.056 mmol/g) [27] also have different operation conditions from those proposed in the present research. At the same time, these are all lower than those previously reported in activated carbons [16,28], zeolites [2], and synthetic materials [29].

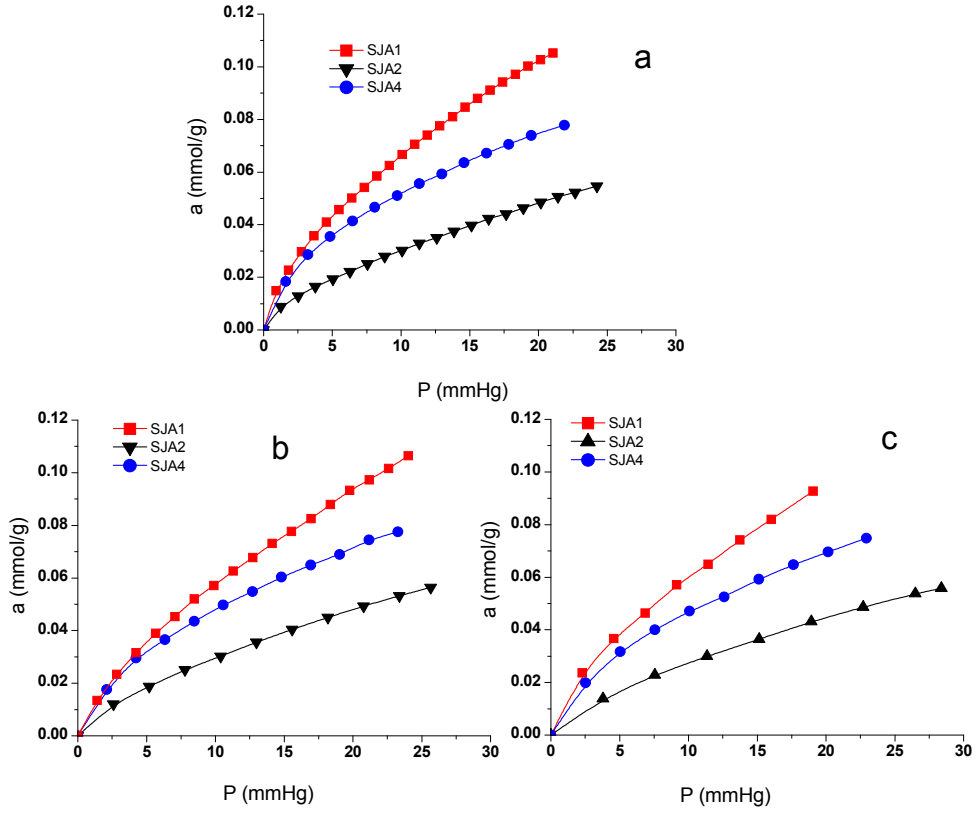

Figure 4. Adsorption isotherms of CO_2 at different temperatures (**a**) 473 K; (**b**) 523 K; and (**c**) 573 K.

The experimental points of the CO_2 isotherms estimated in the interval of 573 to 473 K were evaluated and favorably described for the Freundlich equation in their linear coordinates. It is shown in Figure 5a, with the determination pertinent to the adsorption parameters indicating the heterogeneity in the adsorption sites [30], with correlated coefficients of 0.996 to 0.999. This effect was not observed when the Langmuir equation was applied in these conditions.

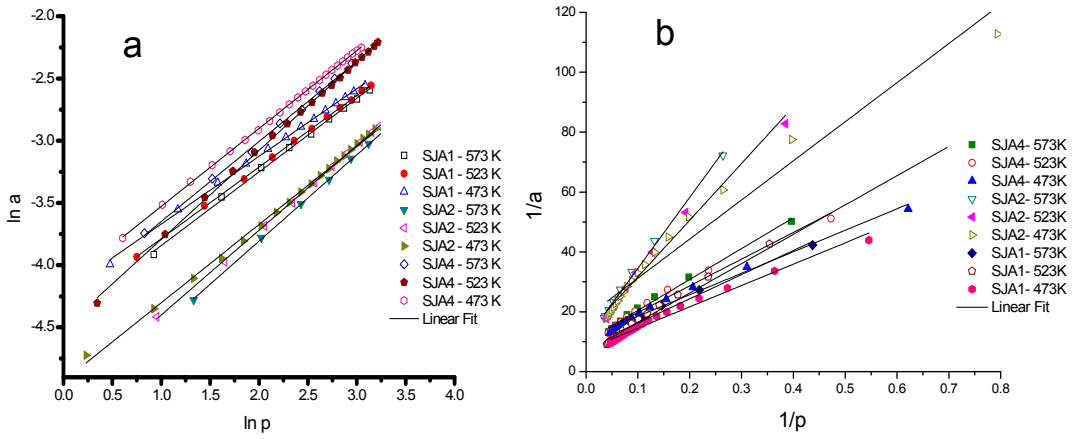

Figure 5. Linear fit of (**a**) the Freundlich model and (**b**) the Langmuir model for the CO_2 adsorption in soils.

The values of the Freundlich constants (K_F) and n, the monolayer adsorption capacity (am), are reported in Table 2. The Langmuir equation considers the interaction of unimolecular unions, and the Freundlich equation is an interactive equation of the adsorbed substance with the adsorbent, which can be related to the element disposition in the soil [22]. The monolayer adsorption capacity (am) and the Langmuir constant (K_L) depend on temperature, deriving from the Langmuir plots (Figure 5b), as shown in Table 3.

Table 3. Freundlich and Langmuir parameters for the adsorption of CO_2 in soils samples with correlation coefficients.

Muestra	T (K)	Freundlich			Langmuir		
		R	n	K_F	R	a_m	K_L
SJA1	573	0.997	1.357	0.0107	0.981	0.152	0.072
	523	0.999	1.398	0.011	0.994	0.149	0.077
	473	0.997	1.598	0.0157	0.972	0.11	0.2
SJA2	573	0.999	1.443	0.0056	0.994	0.092	0.046
	523	0.999	1.47	0.0062	0.984	0.079	0.067
	473	0.999	1.497	0.0064	0.974	0.067	0.088
SJA4	573	0.998	1.691	0.0119	0.992	0.099	0.098
	523	0.999	1.739	0.0128	0.979	0.092	0.121
	473	0.998	1.84	0.0148	0.985	0.088	0.158

The isosteric adsorption heat q_{st} (kJ·mol^{-1}) in low quantities of an adsorbed substance was evaluated from the data of the adsorption isotherms through the Clausius–Clapeyron equation:

$$\left[\frac{\partial \ln p}{\partial T}\right]_a = \frac{q_{st}(a)}{RT^2}, \quad (4)$$

where T and p are the temperature and pressure at equilibrium. In this study, the CO_2 isosteric heats were calculated from the analysis of the linear regression of the graphic p vs. $1/T$ using the

original equilibrium isotherms data [28]. This technique is used at relatively high temperatures as well as for very short times of contact [31] due to the presence of an inactivated diffusion process. The diffusion of CO_2 is hindered by the presence of steric barriers across mesoporous channels; therefore, higher temperatures are required to further permeate these capillaries into the pores beyond [32]. The adsorption isosteric heat shows the energy of interaction among the adsorbate–adsorbent and the adsorbate–adsorbate that take place in the adsorption system. The behavior of the isosteric systems in the studied soils are shown in Figure 6 in which the decline in the isotherm heat of adsorption, in a width interval of the cover surface, can be observed.

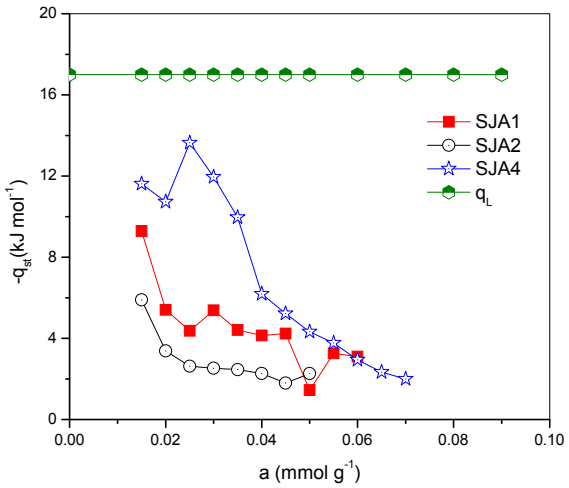

Figure 6. Isoteric heat of CO_2 adsorption of soil samples.

This behavior is frequent on non-uniform surfaces, even when there exist specific adsorbent–adsorbate interactions. In general, in low adsorbed quantities, the isosteric heat magnitude decreases with the addition of adsorbed substance. This behavior is common in adsorbents that have heterogeneous adsorption sites, as in the case of the soil [8].

The thermodynamics parameters in the CO_2 adsorption were evaluated from the data of the adsorption isotherms of Langmuir using the Van't Hoff Equation [33] using the following relations:

$$\Delta G = -RT\ln\frac{p^0}{p}; \quad (5)$$

$$\Delta H = R\frac{T_1T_2}{T_1 - T_2}\ln\frac{P_2}{P_1}; \quad (6)$$

$$\Delta S = \frac{\Delta H - \Delta G}{T}, \quad (7)$$

where ΔG is the free energy change of Gibbs, that is, the same as the isosteric heat under isothermal conditions, leaving behind the gas imperfections, ΔH is the enthalpy change, and ΔS is the entropy change of the adsorption process.

The values of the thermodynamic parameters for the adsorption of CO_2 are presented in Table 4. There, negative values of ΔG are observed, confirming the viability and spontaneous nature of the adsorption process, while the negative values in ΔH indicate that the adsorption phenomenon is exothermic and the positive value of ΔS confirms the affinity [17] of the kaolinite soils toward CO_2.

Table 4. Thermodynamic data for adsorption of CO_2 on SJA1, SJA2 and SJA4.

Muestra	T (K)	$-\Delta H$ (kJ· mol^{-1})	$-\Delta G$ (kJ· mol^{-1})	$-\Delta U$ (kJ· mol^{-1})	ΔS (J· K^{-1}· mol^{-1})
SJA1	573	4.505	71.524	11.491	116.962
	483		55.797		106.193
	453		51.148		102.964
SJA2	573	2.904	69.190	6.648	115.682
	483		55.237		108.352
	453		50.597		105.283
SJA4	573	8.037	70.621	10.394	109.223
	483		55.754		96.413
	453		50.911		102.798

4. Conclusions

The characterization of soils with high kaolinite content was satisfactorily performed through several experimental techniques; the XRD results show that the SJA4 soil contains the crystalline kaolinite phase, while, according to N_2 adsorption, this same sample attained the highest specific surface area and the widest pore size distribution.

The characterization by N_2 adsorption demonstrated the structural heterogeneity of the soil samples studied. For this, it is convenient to conduct studies on pore size distribution. It is necessary not to consider a specific mechanism, but to illustrate the difference between the filling of meso- and macropore surfaces in adsorption processes.

According to the adsorption parameters calculated in this work, CO_2 was favorably adsorbed mainly on the SJA1 sample, which attained the highest values of CO_2 adsorption. This process is physisorption, which can be confirmed by the obtained values of the isosteric heat of adsorption. The adsorption isotherms obtained experimentally were adjusted to the adsorption model of Freundlich, which confirmed the soil heterogeneity and CO_2 multilayer filling for all samples.

However, the transformation of trapped CO_2 into other compounds, such as alcohols, ketones, acids, and aldehydes, seems to have a better end result. After secondary oil recovery, CO_2 can remain buried in the tiny spaces between grains of sand where oil was previously held. CO_2 capture by soils is an important option because of the availability of these substrates.

Author Contributions: Karla Quiroz-Estrada and Miguel Ángel Hernández-Espinosa conceived and designed the experiments; Lucía López, Roberto Portillo and Efraín Rubio performed the experiments; Karla Quiroz-Estrada, Miguel Ángel Hernández-Espinosa and Fernando Rojas analyzed the data and wrote the paper.

Conflicts of Interest: The authors declare no conflict of interest.

References

1. Férey, G.; Serre, C.; Devic, T.; Maurin, G.; Jobic, H.; Llewellyn, P.; De Weireld, G.; Vimont, A.; Daturi, M.; Chang, J. Why hybrid porous solids capture greenhouse gases? *Chem. Soc. Rev.* **2011**, *40*, 550–562. [CrossRef] [PubMed]
2. Maurin, G.; Llewellyn, P.; Bell, R. Adsorption mechanism of carbon dioxide in Faujasites: Grand Canonical Monte Carlo simulations and microcalorimetry measurements. *J. Phys. Chem. B* **2005**, *109*, 16084–16091. [CrossRef] [PubMed]
3. Zhou, J.; Li, W.; Zhang, Z.S.; Xing, W.; Zhuo, S. Carbon dioxide adsorption performance of N-doped zeolite Y templated carbons. *RSC Adv.* **2012**, *2*, 161–167. [CrossRef]
4. Solomon, S.; Qin, D.; Manning, M.; Marquis, M.; Averyt, K.B.; Tignor, M.; Miller, H.L., Jr.; Chen, Z. *Climate Change 2007: The Physical Science Basis: Working Group I Contribution to the Fourth Assessment Report of the IPCC*; Cambridge University Press: Cambridge, UK, 2007; Volume 4.
5. Canadell, J.; Le Quére, C.; Raupach, M.; Field, C.; Buitenhuis, E.; Ciais, P.; Conway, T.; Gillett, N.; Houghton, R.; Marland, G. Contribution to accelerating atmospheric CO_2 growth from economic activity, carbon intensity, and efficiency of natural sinks. *Proc. Natl. Acad. Sci. USA* **2007**, *104*, 18866–18870. [CrossRef] [PubMed]

6. Weber, W.J.; McGinley, P.M.; Katz, L.E. A distributed reactivity model for sorption by soils and sediments. Conceptual basis and equilibrium assessments. *Environ. Sci. Technol.* **1992**, *26*, 1955–1962. [CrossRef]
7. Hernández, M.A.; González, A.I.; Corona, L.; Hernández, F.; Rojas, F.; Asomoza, M.; Solís, S.; Portillo, R.; Salgado, M.A. Chlorobenzene, chloroform, and carbon tetrachloride adsorption on undoped and metal-doped sol-gel substrates SiO_2, Ag/SiO_2, Cu/SiO_2 and Fe/SiO_2. *J. Hazard. Mater.* **2009**, *162*, 254–263. [CrossRef] [PubMed]
8. López, L.; Hernández, M.A.; Ruiz, J.; Carcaño, M.; Medina, G.; Portillo, R.; Muñoz, J. Adsorción de ácidos carboxílicos de origen vegetal y bacteriano en un suelo agrícola. *Terra Latinoam.* **2012**, *30*, 261–270. (In Spanish)
9. Carbon Dioxide Capture and Storage. Available online: https://www.ipcc.ch/report/srccs/ (accessed on 20 June 2016).
10. Bereznitski, Y.; Jaroniec, M.; Maurice, P. Adsorption characterization of two clay minerals society standard kaolinites. *J. Colloid Interface Sci.* **1998**, *205*, 528–530. [CrossRef] [PubMed]
11. Chen, Y.; Lu, D. CO_2 capture by kaolinite and its adsorption mechanism. *Appl. Clay Sci.* **2015**, *104*, 221–228. [CrossRef]
12. Ghosh, D.; Bhattacharyya, K. Adsorption of methylene blue on kaolinite. *Appl. Clay Sci.* **2002**, *20*, 295–300. [CrossRef]
13. Hitch, M.; Li, J. Carbone dioxide sorption isotherm study on pristine and acid-treated olivine and its application in the vacuum swing adsorption process. *Minerals* **2015**, *5*, 259–275.
14. Sen Guptaa, S.; Bhattacharyya, K. Adsorption of heavy metals on kaolinite and montmorillonite: A review. *Phys. Chem. Chem. Phys.* **2012**, *14*, 6698–6723. [CrossRef] [PubMed]
15. Filimonova, S.V.; Knicker, H.; Kögel-Knabner, T.I. Soil micro- and mesopores studied by N_2 adsorption and ^{129}Xe NMR of adsorbed xenon. *Geoderma* **2006**, *130*, 218–228. [CrossRef]
16. Hauchhum, L.; Mahanta, P. Carbon Dioxide adsorption on zeolites and activated carbon by pressure swing adsorption on a fixed bed. *Int. J. Energy Environ. Eng.* **2014**, *5*, 349–356. [CrossRef]
17. Plaza, M.; Pevida, C.; Pis, J.; Rubiera, F. Evaluation of the cyclic capacity of low-cost carbon adsorbents for post- combustion CO_2 capture. *Energy Proced.* **2011**, *4*, 1228–1234. [CrossRef]
18. Pacala, S.; Socolow, R. Stabilization wedges: Solving the climate problem for the next 50 years with current technologies. *Science* **2004**, *305*, 968–972. [CrossRef] [PubMed]
19. Hernández, M.A.; Quiroz, K.; Rojas, F.; Portillo, R.; Salgado, M.; Hernández, F.; Rivera, A. Experiment and modeling of low coverage uptake of N_2 and O_2 on H-clinoptilolite zeolite from Tehuacán, Puebla, Mexico. *J. Chem. Chem. Eng.* **2014**, *8*, 1–10.
20. Schaef, H.; Glezakou, V.; Owen, A.; Ramprasad, S.; Martin, P.; McGrail, B. Surface condensation of CO_2 onto kaolinite. *Environ. Sci. Technol. Lett.* **2014**, *1*, 142–145. [CrossRef]
21. Hernández, M.A.; Portillo, R.; Salgado, M.A.; Rojas, F.; Petranoskii, V.; Pérez, G.; Salas, R. Comparación de la capacidad de adsorción de CO_2 en clinoptilolitas naturales y tratadas químicamente. *Superf. Vacío* **2010**, *23*, 67–72. (In Spanish)
22. Choudary, V.R.; Mantri, K. Adsorption of aromatic hydrocarbons on highly siliceous MCM-41. *Langmuir* **2000**, *16*, 7031–7037. [CrossRef]
23. Petacek, P.; fuvátová, D.; Havlica, J.; Brandstetr, J.; Soukal, F.; Opravil, T. Isothermal kinetic analysis of the thermal decomposition of kaolinite: The thermogravimetric study. *Thermochim. Acta* **2010**, *501*, 24–29. [CrossRef]
24. Meroufel, B.; Benali, O.; Benyahia, M.; Benmoussa, Y.; Zenasni, M.A. Adsorptive removal of anionic dye from aqueous solutions by Algerian kaolin: Characteristics, isotherm, kinetic and thermodynamic studies. *J. Mater. Environ. Sci.* **2013**, *4*, 482–491.
25. Besoain, E. Mineralogía de Arcillas de Suelo. Minerales secundarios del suelo: Silicatos cristalinos. In *Mineralogia de Arcillas de Suelos*; Escoto, J., Ed.; IICA: San José, Costa Rica, 1985; Volume 1, pp. 311–533. (In Spanish)
26. Volzone, C.; Thompson, J.G.; Melnitchenko, A.; Ortiga, J.; Palothorpe, R.S. Selective gas adsorption by amorphous clay mineral derivatives. *Clays Clay Miner.* **1999**, *47*, 647–657. [CrossRef]
27. Melnitchenko, A.; Thompsion, J.; Volzone, C.; Ortiga, J. Selective gas adsorption by metal exchanged amorphous kaolinite derivatives. *Appl. Clay Sci.* **2000**, *17*, 35–53. [CrossRef]

28. Yuan, B.; Wu, X.; Chen, Y.; Huang, J.; Luo, H.; Deng, S. Adsorption of CO_2, CH_4, and N_2 on ordered mesoporous carbon: Approach for greenhouse capture and biogas upgrading. *Environ. Sci. Technol.* **2013**, *47*, 5474–5480. [CrossRef] [PubMed]
29. Hutson, N.; Speakman, S.; Payzant, A. Structural effects on the high temperature adsorption of CO_2 on a synthetic hydrotalcite. *Chem. Mater.* **2004**, *16*, 4135–4143. [CrossRef]
30. Ng, C.; Losso, J.N.; Marshall, W.E.; Rao, R.M. Freundlich adsorption isotherms of agricultural by-product-based powdered activated carbons in a geosmin–water system. *Bioresour. Technol.* **2002**, *85*, 131–135. [CrossRef]
31. Hernández, M.A.; Velasco, J.; Rojas, F.; Campos, E.; Lara, V.; Torres, J.; Salgado, M. Adsorción de compuestos orgánicos volátiles en arcillas del estado de Puebla, México. *Rev. Int. Contam. Ambient.* **2003**, *19*, 191–196. (In Spanish)
32. Hernández, M.A.; Corona, L.; González, A.I. Quantitative study of the adsorption of aromatic hydrocarbons (Benzene, Toluene, and *p*-Xylene) on dealuminated clinoptilolites. *Ind. Eng. Chem. Res.* **2005**, *44*, 2908–2916. [CrossRef]
33. Alzaydien, A.S.; Manasreh, W. Equilibrium, kinetic and thermodynamic studies on the adsorption of phenol onto activated phosphate rock. *Int. J. Phys. Sci.* **2009**, *4*, 172–181.